

All-Optical Analog-to-Digital Converters, Hardlimiters, and Logic Gates

Lukasz Brzozowski and Edward H. (Ted) Sargent

Abstract—The authors propose and analyze the optical signal processing functionality of periodic structures consisting of alternating layers of materials possessing different Kerr nonlinearities. They explore structure–materials–performance relationships in all-optical analog-to-digital converters, hardlimiters, and AND and OR gates. They show that their proposed analog-to-digital converters can extract a binary word from multilevel optical signals in a single bit interval. They also propose a family of optical limiters whose output signal clamps to a set upper logic level for any input value exceeding a chosen threshold. They explore the performance of an all-optical logic gate whose forward-directed output implements a binary AND and whose backward-directed output implements an OR function.

Index Terms—Analog-to-digital converter, gates, hardlimiter, Kerr nonlinearity, logic, nonlinear optics, optical bistability, optical switching, optical signal processing.

I. INTRODUCTION

THE EMERGENCE of increasingly high-speed, parallel, and complex digital optical systems demands an all-optical analog-to-digital converter. At the same time, optical hardlimiters are needed in synchronous and asynchronous optical code-division multiple-access (CDMA) systems [1], [2]. Limiters also form a prospective basis for all-optical logic.

Present-day electronic signal processing speeds have fallen far behind the capabilities of both optical time-division and wavelength division multiplexed (WDM) systems. Electrical-to-optical and optical-to-electrical conversions limit the speed and sophistication of photonic networks [3]. On the other hand, performing signal processing operations entirely within the optical domain would exploit the speed and parallelism inherent to optics.

We propose and explore herein a set of principles and device architectures which could enable the realization of an array of optical signal processing functions. The devices rely upon the mechanism of nonlinear reflection rather than absorption of light and are, as such, less susceptible to damage than absorption-based devices [4], [5]. Composed of formable multilayer structures, the devices are relatively easy to fabricate into a desired shape or to attach to any kind or form of surface.

For illustrative purposes, we restrict our analysis in the present work to the case of a one-dimensional (1-D) periodic nonlinear model system. A vast array of further device opportunities arises in the context of periodic three-dimensional (3-D) media. Such structures have already been realized through

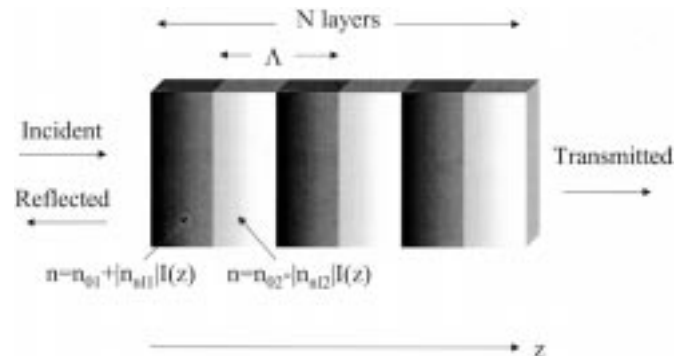


Fig. 1. Structures consisting of alternating layers of materials with different linear refractive indexes and Kerr coefficients.

techniques of mesoscopic self-organization both in inorganic [6] and organic [7] materials. Either system lends itself to the selective inclusion of materials with fast Kerr-type nonlinearities of opposite signs. Devices which are either angularly and spectrally broadband or narrowband can be realized in these regular media. Signal-processing elements rooted not simply in 1-D nonlinear distributed reflection, but implementing nonlinear diffraction of signals—mediated by the set of available reciprocal photonic lattice vectors—can be envisioned.

Self-organization of bulk samples is extensible to the domain of two-dimensional (2-D) confined systems—i.e., ordering of monodisperse mesoparticles inside the cylindrical core of an optical fiber. This would enable a class of connectorized, low-loss, functional photonic devices.

II. THEORETICAL MODEL

The structures analyzed are shown in Fig. 1. They consist of alternating layers of materials, each one possessing a Kerr nonlinearity. The index of refraction of such a material can be expressed as [8], [9]

$$n = n_0 + n_{nl}I \quad (1)$$

where

- n_0 linear index;
- n_{nl} Kerr coefficient;
- I local intensity of light in the medium.

Depending on the material and optical wavelength, the index of refraction may either increase or decrease with intensity [10], [11], as embodied in the sign of n_{nl} .

In general, a nonlinear distributed feedback structure may display multistability [12]–[18]. In a multistable device there are at least two possible outputs for a range of choices of incident

intensity. Moreover, the spectral position of the transmittance minimum shifts as the incident intensity is varied. Multistable structures do not exhibit saturation of the transmitted intensity to a limiting value and may manifest chaotic behavior [14]. Such a response is undesirable in analog-to-digital converters and hardlimiters. We derive the conditions that ensure the stability of nonlinear distributed feedback structures.

In analogy with the case of linear periodic structures [19], the Bragg condition for a medium with intensity-dependent refractive indexes is itself a function of intensity

$$(n_{01} + n_{n1}I) d_1 + (n_{02} + n_{n2}I) d_2 = \frac{\lambda}{2} \quad (2)$$

where

- n_{01} and n_{02} linear parts of the refractive indexes of the two materials;
- n_{n1} and n_{n2} Kerr coefficients;
- d_1 and d_2 corresponding layer thicknesses.

The spectral position λ of the center of the stopband of a periodic grating is given by (2).

With a view to achieving stable, narrowband device operation, we require that the center of the stopband stay fixed in the intensity-dependent medium, so that

$$n_{01}d_1 + n_{02}d_2 = \frac{\lambda}{2} \quad (3)$$

$$n_{n1}d_1 + n_{n2}d_2 = 0. \quad (4)$$

This condition can be fulfilled only if the Kerr coefficients are of opposite sign. We solve (4) and (5) for d_1 and d_2

$$d_1 = \frac{\lambda}{2 \left(n_{01} - n_{02} \frac{n_{n1}}{n_{n2}} \right)} \quad (5)$$

$$d_2 = \frac{\lambda}{2 \left(n_{02} - n_{01} \frac{n_{n2}}{n_{n1}} \right)}. \quad (6)$$

Expressions (5) and (6) specify the thicknesses of the layers which, for a given pair of nonlinear materials, ensure the stability of the system, fixing the transmittance minimum at λ regardless of incident intensity. Equations (2), (5), and (6) are heuristic: in reality, the intensity will vary from layer to layer, but only slowly between adjacent layers in low-index-contrast structures, in which case the approximation is a good one. Results obtained through exact methods and reported later in this work confirm that fulfillment of these conditions results in a stable response.

In order to model the response of the proposed structures, we adapt the coupled mode equations [19] to the case of a nonlinear medium. We write the electromagnetic field as a sum of forward and backward propagating waves

$$E(z) = A_1(z)e^{ikz} + A_2(z)e^{-ikz} \quad (7)$$

where A_1 and A_2 are the forward- and backward-propagating wave envelopes and k is the propagation constant.

We analyze the case of noncoherent radiation wherein intensity, proportional to the squared modulus of the electric field, is approximated as $I(z) = |A_1(z)|^2 + |A_2(z)|^2$ [8]. We then expand the periodic linear and nonlinear parts of the index of refraction in Fourier series [18]

$$n(z) = n_0 + (n_1 - n_2)f(z) \quad (8)$$

$$n_{nl}(z) = n_{nl0} + (n_{nl1} - n_{nl2})f(z) \quad (9)$$

where $n_0 = (n_{01}d_1 + n_{02}d_2)/\Lambda$ and $n_{nl0} = (n_{nl1}d_1 + n_{nl2}d_2)/\Lambda$ are average linear and nonlinear refractive indexes, Λ is the period of the grating, and

$$f(z) = \sum_{m \neq 0} \exp(im\pi X) \frac{\sin m\pi X}{m\pi} \exp\left(i \frac{2m\pi z}{\Lambda}\right). \quad (10)$$

is the Fourier expansion of the step function with $X = d_1/\Lambda$.

Since we analyze device response near the structural resonance [i.e., conditions (5) and (6) satisfied], only the first-order terms take part in the contradirectional coupling. The higher order Fourier coefficients do not result in phase matching. We have verified through full numerical solution of the exact equation set that the inclusion of these higher order terms results in no noticeable changes to the transfer curves. By restricting our attention to the pertinent Fourier component, we thus obtain coupled mode equations for a nonlinear periodic structure with negligible absorption

$$\begin{aligned} i \frac{dA_1(z)}{dz} &= \frac{\omega}{c} \left\{ \left[(n_{01} - n_{02}) + (n_{n1} - n_{n2})I(z) \right] \right. \\ &\quad \cdot \exp\left(-i \frac{\pi d_2}{\Lambda}\right) \frac{\sin \frac{\pi d_2}{\Lambda}}{\pi} A_2(z) \\ &\quad \left. \cdot \exp\left[i \left(\frac{2\omega n_0}{c} - \frac{2\pi}{\Lambda} \right) z\right] - \bar{n}_{nl}I(z)A_1(z) \right\} \end{aligned} \quad (11)$$

$$\begin{aligned} i \frac{dA_2(z)}{dz} &= -\frac{\omega}{c} \left\{ \left[(n_{01} - n_{02}) + (n_{n1} - n_{n2})I(z) \right] \right. \\ &\quad \cdot \exp\left(i \frac{\pi d_2}{\Lambda}\right) \frac{\sin \frac{\pi d_2}{\Lambda}}{\pi} A_1(z) \\ &\quad \left. \cdot \exp\left[-i \left(\frac{2\omega n_0}{c} - \frac{2\pi}{\Lambda} \right) z\right] - \bar{n}_{nl}I(z)A_2(z) \right\} \end{aligned} \quad (12)$$

where ω is the frequency of the radiation and c is the speed of light in vacuum.

We specify two boundary conditions: $A_2(L) = 0$ (no radiation incident on the structure from the right) and $|A(0)|^2 = I_{\text{in}}$ (known intensity incident on the structure from the left).

III. RESULTS AND DISCUSSION

Aided by coupled equations (11) and (12), we proceed to explore potential uses of the proposed structures as all-optical functional components in photonic networks. We propose hardlimiters, analog-to-digital converters, and OR and AND gates based on our generic structure.

We show in Fig. 2 the transmitted intensity of the periodic nonlinear medium as a function of incident intensity for various numbers of layers. Here and in the rest of the paper we consider light of wavelength at the center of the linear stopband chosen according to conditions (5) and (6). The structures analyzed are made up of materials with the linear indexes of refraction of 1.5 and 1.52 and Kerr coefficients of 0.01 and -0.01 . Throughout this work we consider intensity in units reciprocal to those of n_{nl} . We observe in Fig. 2 three regimes of operation: at low intensities, the incident signal is resonantly reflected; for intermediate incident intensity, the system goes through a region of constant differential transmittance; for high incident intensity, the transmittance redescends to zero.

We illustrate in Fig. 3 the mechanisms responsible for this behavior. We plot the evolution of intensity and the intensity-dependent refractive index for various values of I_{in} across the 500-period structure with the same material parameters as in Fig. 2. Low incident intensity ($I_{in} = 0.3$) is blocked by the strong linear grating and decays to a negligible value in the first part of the structure. As the intensity is increased beyond $(n_{01} - n_{02})/2(|n_{nl1}| + |n_{nl2}|)$ the nonlinearity modifies substantially the profile of refractive index variation across the structure ($I_{in} = 0.65$). Since the layers with higher linear index have a negative Kerr coefficient, and those with lower n_0 have a positive n_{nl} , increasing intensity initially decreases the difference between the total indexes of refraction, reducing the net amplitude of the grating. The transmitted intensity is no longer zero. When the incident intensity reaches $(n_{01} - n_{02})/(|n_{nl1}| + |n_{nl2}|)$, the grating disappears and the structure is completely transmitting. As the incident intensity is increased further ($I_{in} = 1.07$) the grating (phase-shifted relative to the initial linear grating) forms again, resulting in the limiting behavior manifest in Fig. 2. The transmitted intensity is clamped at $(n_{01} - n_{02})/2(|n_{nl1}| + |n_{nl2}|)$. In order to achieve such sharp characteristics, the structures analyzed need to be at least 500 periods long.

We show in Fig. 4 the response of structures with strong built-in linear stopband (large number of layers or high linear index contrast) for different materials (different n_0 and n_{nl}). We define a new parameter a

$$a = \frac{n_{01} - n_{02}}{|n_{nl1}| + |n_{nl2}|}. \quad (13)$$

For a given choice of materials (a), the transmitted intensity (I_{out}) is related to incident intensity by the approximate piecewise-linear relation:

$$I_{out} = \begin{cases} 0, & \text{for } I_{in} < \frac{a}{2} \\ 2a(I_{in} - 1), & \text{for } \frac{a}{2} < I_{in} < a \\ a, & \text{for } I_{in} > a. \end{cases} \quad (14)$$

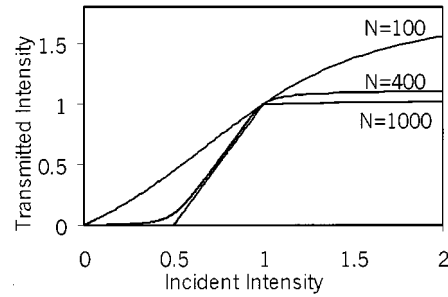


Fig. 2. Transmitted intensity for the structures for various numbers of layers. The structures have linear refractive indexes of 1.5 and 1.52 and Kerr coefficients of 0.01 and -0.01 .

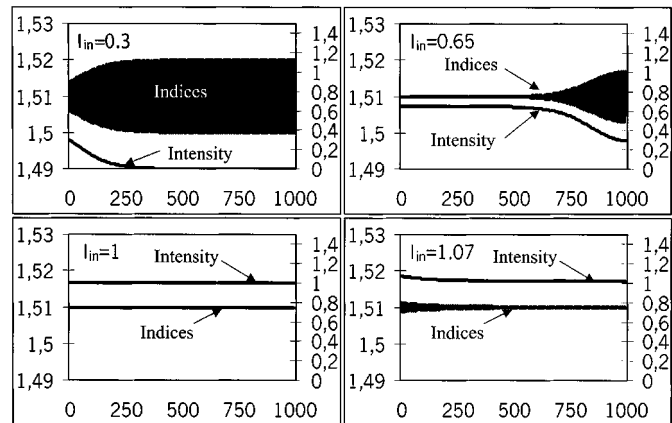


Fig. 3. Local index and intensity across a 500-period structure with material parameters as in Fig. 2 for various values of incident intensity. Total refractive index is given on the left vertical axis and intensity is given on the right axis.

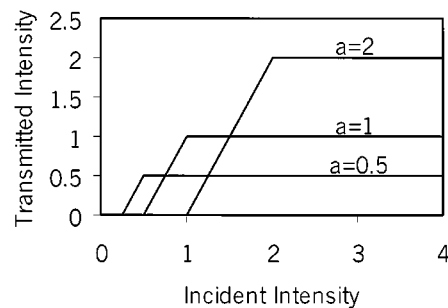


Fig. 4. Transmitted intensity for structures made of different materials. The limiting value changes according to the magnitude of linear and nonlinear parts of indexes of refraction $a = (n_{01} - n_{02})/(|n_{nl1}| + |n_{nl2}|)$.

As the strength of the linear grating weakens (short structures or low linear index contrast) the transmission characteristics deviate near $I_{in} = a/2$ and $I_{in} = a$ from the values defined by 14.

In a hardlimiter the output should be one for input greater than or equal to one, and should otherwise be zero [1], [2]. We illustrate in Fig. 5 the realization using the proposed structures of an all-optical hardlimiter with arbitrarily steep transition stages. N limiters with $a = 1$ are positioned in series, with optical isolators between each pair. These isolators allow light to propagate in the forward direction and absorb reflected light. The first nonlinear grating blocks show incident radiation with intensity smaller than $a/2$. However, the transmitted intensity still ranges from 0 to a . This light is then fed into the second unit, and again

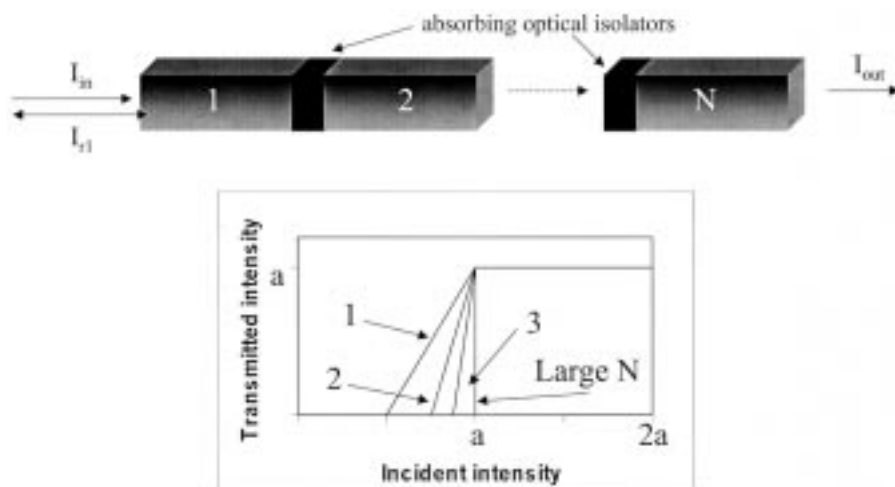


Fig. 5. All-optical hardlimiter. Arranging the proposed structures in series results in an increasingly steep transition. The configuration employs optical isolators. The insert shows the how the response of the hardlimiter is modified with the increasing number of units.

light with intensity lower than $a/2$ is blocked. Light with intensity lower than $a/2$ seen by the second unit corresponds to light incident on the composite device with intensity larger than $a/2$ and lower than $3a/4$. Generalizing for N , we obtain the following transmission characteristic:

$$I_{\text{out}} = \begin{cases} 0, & \text{for } I_{\text{in}} < a \left(1 - \frac{1}{2^N}\right) \\ a[2^N(I_{\text{in}} - 1) + 1], & \text{for } a \left(1 - \frac{1}{2^N}\right) < I_{\text{in}} < a \\ a, & \text{for } I_{\text{in}} > a. \end{cases} \quad (15)$$

Thus, given a sufficiently large number of units, the proposed device will behave as an arbitrarily abrupt all-optical hardlimiter. All of the intensities smaller than a will be reflected and all greater or equal to a will be transmitted. The transmitted intensities will clamp to a . Since the value of a is determined by linear and nonlinear indexes, the choice of material biases the device at the desired value.

We illustrate in Fig. 6 a four-bit analog-to-digital converter constructed using the limiters described above. Our approach is scalable to higher resolutions. The n th additional bit requires $n - 1$ limiters. The total number of limiters for an N -level A-D converter is $N(N - 1)/2$. Delay lines can be placed along the output lines to ensure that all signals arrive at the receiver simultaneously. The separation of the incident and reflected signals can be performed with nonreciprocal directional couplers [20], [21].

The analog-to-digital converter illustrated in Fig. 6 is constructed using limiters biased at values 8, 4, and 2. As an example we illustrate A/D conversion of analog input 5. 5 is fully reflected by the first set of limiters (fourth level) giving an output of 0. In the third level, 4 is transmitted and 1 reflected. The 4 output is normalized to yield the second digital output, 1. The reflected 1 is fed into the second level and is completely reflected. The 0 at the output of the second level provides the third digit. Signal 1 reflected from the second level yields the lowest order digit. Placing delay lines behind second, third, and fourth levels ensures that the four digital signals arrive simultaneously at the

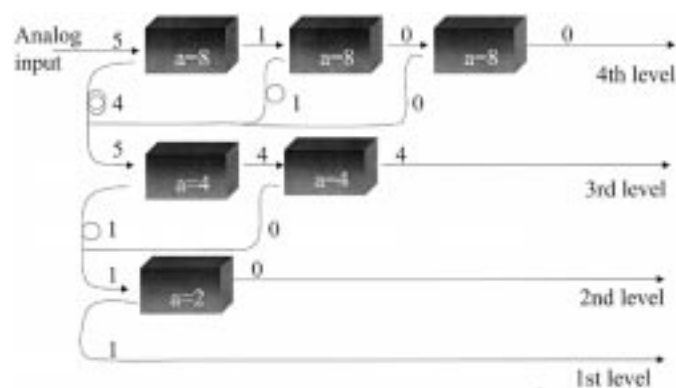


Fig. 6. All-optical analog-to-digital converter. In the example considered, an analog input of 5 is transformed to the digital word (0101).

corresponding receivers. An analog input of 5 is converted to a (0101) digital word in a single byte interval. Our approach provides a basis for all-optical, ultrafast decoding of multi-amplitude intensity signals [22].

We illustrate in Fig. 7 the use of the proposed limiter in the construction of OR and AND gates. Inputs A and B are first combined into a single beam. The transmitted intensity is defined as the O1 output and the reflected value as the O2. We bias the hardlimiter at 1. If one of the inputs is 0 and the other 1, the output at O1 is 1 and at O2 is 0. If both A and B inputs have the value of 1, a 1 is transmitted and 1 reflected. Thus, O1 yields the result of an OR operation and O2 the result of a digital AND.

Implementation of the devices considered herein will rely on the use of materials with large Kerr nonlinearities in order to obtain a low-intensity threshold for limiting action. Recently, highly nonlinear materials with low absorption coefficients have been reported with n_{nl} ranging from 1×10^{-10} cm^2/W to as high as 1×10^{-6} cm^2/W with response times of picoseconds or better [10]–[12], [23]–[25]. A 1-mm-long limiter operating on $0.532 \mu\text{m}$ light would, using these materials, achieve switching and limiting intensities of 1×10^6 W/cm^2 to as low as 1×10^2 W/cm^2 . These intensities are many orders of magnitude lower than reported for reverse saturable absorption-based limiters of

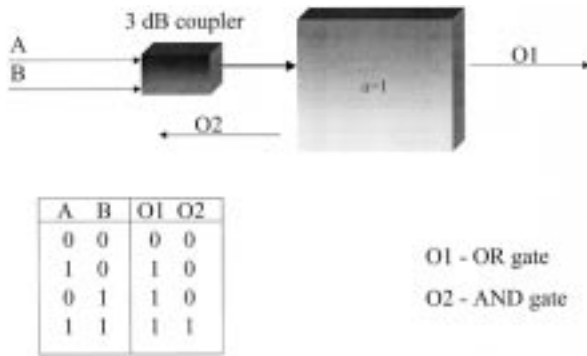


Fig. 7. OR and AND gates. For two input beams A and B, the transmitted intensity of the hardlimiter biased at 1 implements the OR function while the reflected beam implements the AND operation.

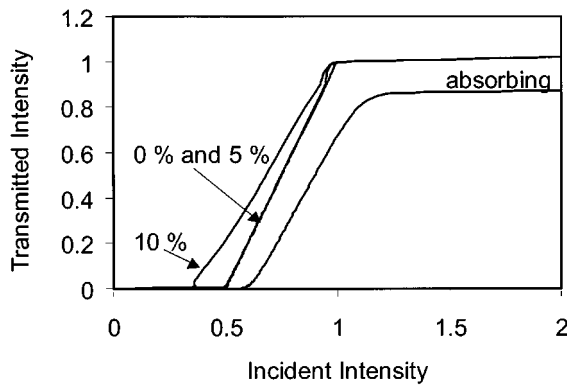


Fig. 8. Transmitted intensity as a function of incident intensity for the structure with the same parameters as in Fig. 3. The thickness of the layers was allowed to vary 0, 5, and 10% from their quarter-wave value. The effect of linear absorption of 6 cm^{-1} on transmittance is also shown.

the same length and operating at the same wavelength. These typically require incident intensity of the order of 0.1 GW/cm^2 and do not exhibit full clamping of the transmitted intensity [36, 37, 38]. The necessity of using a large number of periods in order to achieve low switching intensities raises the possibility of linear absorption: in fact, a 1-mm-long sample fabricated using the materials discussed above would result in lowering the maximum (linearly) transmitted intensity to 90%. The qualitative behavior of the proposed devices is preserved in the presence of such realistic absorption, as illustrated in Fig. 8, in which we take the absorption coefficient to be 6 cm^{-1} .

In addition to presenting potential uses of the proposed structures in signal processing, we analyze their sensitivity to realistic imperfections incurred during fabrication. We simulate the response of structures with built-in random fluctuations in the layer thicknesses. Keeping all other parameters fixed, we allow the thicknesses to be distributed uniformly over a predefined range. In Fig. 8 we show the transmitted intensity as a function of incident intensity for the structure with the same average parameters as in Fig. 7. Layer thicknesses were allowed to vary 5 and 10% from their quarter-wave value. For 5% deviation there is no detectable difference in the responses of the imperfect device and the ideal device. Even in devices with larger degrees of

imperfection (10% fluctuations) the transmitted intensity saturates to some limiting value. Thus, though the quantitative performance of the device is affected by fabrication errors, pertinent qualitative features of device behavior are preserved.

IV. CONCLUSION

The structures which we have proposed herein are suitable for realization of all-optical devices with applications in photonic networks. We describe using simplified analytical expressions the relationships between device behavior and underlying material and structural characteristics. Aided by the analytical expressions derived and numerical simulations employed, we quantify the performance of our structures as all-optical hardlimiters. We have demonstrated that the proposed devices would maintain key qualitative behavior even with substantial fabrication errors. We present the use of these hardlimiters in realization of A/D converters and logic gates.

ACKNOWLEDGMENT

The authors thank E. Johnson.

REFERENCES

- [1] T. Ohtsuki, K. Sato, I. Sasase, and S. Mori, "Direct-detection CDMA systems with double optical hard-limiters using modified prime sequence codes," *IEEE J. Select. Areas Commun.*, vol. 14, pp. 1879–1887, Dec. 1996.
- [2] T. Ohtsuki, "Performance analysis of direct-detection optical asynchronous CDMA systems with double optical hard-limiters," *IEEE J. Lightwave Technol.*, vol. 14, pp. 452–457, Mar. 1997.
- [3] J. M. Senior, *Optical Fiber Communications, Principles and Practice*, 2nd ed. Cambridge, U.K.: Cambridge Univ. Press, 1992.
- [4] R. C. Hollins, "Overview of research on nonlinear optical limiters at DERA (Defence Evaluation & Res. Agency, Malvern, UK)," *SPIE: Photosensitive Optical Materials and Devices II*, vol. 3292, pp. 2–8, June 1988.
- [5] G. L. Wood, W. W. Clark III, M. J. Miller, G. J. Salamo, and E. J. Sharp, "Evaluation of passive optical limiters and switches," *SPIE: Materials for Optical Switches, Isolators, and Limiters*, vol. 1105, pp. 154–181, Aug. 1989.
- [6] I. Sokolov, H. Yang, G. A. Ozin, and C. T. Kresge, "Radial patterns in mesoporous silica," *Advanced Materials*, vol. 11, no. 8, pp. 636–642, June 2, 1999.
- [7] E. Kumacheva, O. Kalinina, and L. Lige, "Three-dimensional arrays in polymer nanocomposites," *Advanced Materials*, vol. 11, no. 3, pp. 231–234, Feb. 11, 1999.
- [8] B. E. A. Saleh and M. C. Teich, *Fundamentals of Photonics*. New York: Wiley, 1991.
- [9] G. I. Stegeman, C. Liao, and H. G. Winful, "Distributed feedback bistability in channel waveguides," in *Optical Bistability 2*, C. M. Bowden, H. M. Gibbs, and S. L. McCall, Eds. New York: Plenum, 1983, pp. 389–396.
- [10] R. Rangel-Rojo, S. Yamada, S. Matsuda, and H. D. Yankelevich, "Large near-resonance third-order nonlinearity in an azobenzene-functionalized polymer film," *Appl. Phys. Lett.*, vol. 72, no. 9, pp. 1021–1023, Mar. 1998.
- [11] H. S. Nalwa and S. Miyata, *Nonlinear Optics of Organic Molecules and Polymers*. Boca Raton, FL: CRC, 1999.
- [12] P. W. Smith, "Bistable optical devices promise subpicosecond switching," *IEEE Spectrum*, pp. 26–33, June 1981.
- [13] H. G. Winful, J. H. Marburger, and E. Garmire, "Theory of bistability in nonlinear distributed feedback structure," *Appl. Phys. Lett.*, vol. 35, no. 5, pp. 379–381, Sept. 1979.
- [14] H. G. Winful and G. D. Cooperman, "Self-pulsing and chaos in distributed feedback bistable optical devices," *Appl. Phys. Lett.*, vol. 40, no. 4, pp. 298–300, Feb. 1982.
- [15] C. X. Shi, "Optical bistability in reflective fiber grating," *IEEE J. Quantum Electron.*, vol. 31, pp. 2037–2043, Nov. 1995.

- [16] H. M. Gibbs, *Optical Bistability: Controlling Light with Light*. Orlando, FL: Academic, 1985.
- [17] S. Dubovitsky and W. H. Steier, "Analysis of optical bistability in a nonlinear coupled resonator," *IEEE J. Quantum Electron.*, vol. 28, pp. 585–589, Mar. 1992.
- [18] J. He and M. Cada, "Optical bistability in semiconductor periodic structures," *IEEE J. Quantum Electron.*, vol. 27, pp. 1182–1188, May 1991.
- [19] A. Yariv and P. Yeh, *Optical Waves in Crystals*. New York: Wiley, 1984.
- [20] S. Trillo and S. Wabnitz, "Nonlinear nonreciprocity in a coherent mismatched directional coupler," *Appl. Phys. Lett.*, vol. 49, no. 13, pp. 752–754, Sept. 1986.
- [21] M. S. Whalen and T. H. Wood, "Effectively nonreciprocal evanescent-wave optical-fiber directional coupler," *Electron. Lett.*, vol. 21, no. 5, pp. 175–176, Feb. 1985.
- [22] B. P. Lathi, *Modern Digital and Analog Communication Systems*. Orlando, FL: Dryden, 1989.
- [23] Z. X. Zhang, W. Qiu, E. Y. B. Pun, P. S. Chang, and Y. Q. Shen, "Doped polymer films with high nonlinear refractive indices," *Electron. Lett.*, vol. 32, no. 2, pp. 129–130, Jan. 1996.
- [24] C. R. Mendoca, M. M. Costa, J. A. Giacometti, F. D. Nunes, and S. C. Zilio, "Nonlinear refractive indices of polystyrene films doped with azobenzene dye Disperse Red 1," *Electron. Lett.*, vol. 34, no. 1, pp. 116–117, Jan. 1998.
- [25] W. Van Stryland and M. Shei-Bahae, "Z-Scan," *Characterization Techniques and Tabulations for Organic Nonlinear Optical Materials*, M. G. Kuzyk and C. W. Dirk, Eds. New York: Marcel Dekker, 1998, pp. 655–692.



Lukasz Brzozowski was born in Poland in 1976, and received the B.Sc. degree (Honors, with High Distinction) with a specialization in Physics and Mathematical Sciences from the University of Toronto, Canada, in April 1999.

He is currently pursuing the Ph.D. degree in the Department of Electrical and Computer Engineering, University of Toronto, as a member of Prof. E. H. Sargent's group. During the summer of 2000, he held the position of Visiting Scientist at the Laboratoire Photonique Quantique et Moléculaire of the Ecole Normale Supérieure de Cachan, Paris, France.

Mr. Brzozowski holds a Postgraduate Scholarship from Canada's National Sciences and Engineering Research Council.



Edward H. (Ted) Sargent holds the Nortel Junior Chair in Emerging Technologies in the Department of Electrical and Computer Engineering at the University of Toronto, Canada. He leads a group of 12 graduate and postdoctoral researchers in the areas of semiconductor quantum electronic devices, photonic crystal applications, hybrid organic inorganic quantum dot electroluminescence, and multiple-access optical networks.

Prof. Sargent was awarded the Silver Medal of the Natural Sciences and Engineering Research Council of Canada for his work on the lateral current injection laser and the Premier's Research Excellence Award in recognition of research into the application of photonic crystals in lightwave systems, both in 1999.